

Available online at [www.sciencedirect.com](http://www.sciencedirect.com)

# Resuscitation Plus

journal homepage: [www.elsevier.com/locate/resuscitation-plus](http://www.elsevier.com/locate/resuscitation-plus)

## Experimental paper

# Carbon monoxide-releasing molecule-3 exerts neuroprotection effects after cardiac arrest in mice: A randomized controlled study

Yuanrui Zhao<sup>a,b</sup>, Zhun Yao<sup>a,b</sup>, Liping Lu<sup>a</sup>, Song Xu<sup>a</sup>, Jianfei Sun<sup>a,b</sup>, Ying Zhu<sup>a,b</sup>, Yanping Wu<sup>a,b</sup>, Zhui Yu<sup>a,\*</sup>

### Abstract

**Background:** Post-cardiac arrest brain injury (PCABI) is the leading cause of death in survivors of cardiac arrest (CA). Carbon monoxide-releasing molecule (CORM-3) is a water-soluble exogenous carbon monoxide that has been shown to have neuroprotection benefits in several neurological disease models. However, the effects of CORM-3 on PCABI is still unclear.

**Methods:** A mice model combined asystole with hemorrhage was used. Mice were anesthetized and randomized into 4 groups (n = 12/group) and underwent either 9.5 min CA followed by cardiopulmonary resuscitation (CPR) or sham surgery. CORM-3 (30 mg/kg) or vehicle (normal saline) were administered at 1 h after return of spontaneous circulation or sham surgery. Survival, neurologic deficits, alterations in the permeability of the brain-blood barrier and cerebral blood flow, changes of oxidative stress level, level of neuroinflammation and neuronal degeneration, and the activation of Nrf2/HO-1 signaling pathway were measured.

**Results:** In CORM-3 treated mice that underwent CA/CPR, significantly improved survival (75.00% vs. 58.33%,  $P = 0.0146$  (24 h) and 66.67% vs. 16.67%,  $P < 0.0001$  (72 h)) and neurological function were observed at 24 h and 72 h after ROSC ( $P < 0.05$  for each). Additionally, increased cerebral blood flow, expression of tight junctions, and reduced reactive oxygen species generation at 24 h after ROSC were observed ( $P < 0.05$  for each). CORM-3 treated mice had less neuron death and alleviated neuroinflammation at 72 h after ROSC ( $P < 0.05$  for each). Notably, the Nrf2/HO-1 signaling pathway was significantly activated in mice subjected to CA/CPR with CORM-3 treatment.

**Conclusions:** CORM-3 could improve survival and exert neuroprotection after CA/CPR in mice. CORM-3 may be a novel and promising pharmacological therapy for PCABI.

**Keywords:** Carbon monoxide-releasing molecule-3, Cardiac arrest, Post-cardiac arrest brain injury, Neuroprotection, Carbon monoxide

## Introduction

Cardiac arrest (CA) is a prevalent and significant public health concern with a high mortality rate.<sup>1</sup> Patients who achieve returned of spontaneous circulation (ROSC) after cardiopulmonary resuscitation (CPR) may develop post-CA brain injury (PCABI), myocardial dysfunction, systemic ischemia–reperfusion injury (IRI), and persistent precipitating pathophysiology, collectively termed post-cardiac arrest syndrome.<sup>2,3</sup> The brain function largely depends on the oxygen supply so that brain is more susceptible to ischemia than the other organs. Cerebral blood flow (CBF) ceases when CA occurs, and then the primary ischemia injury starts.<sup>4,5</sup> After that, the brain experiences

“low flow” state during CPR and “reflow” state after ROSC, both of which would worsen neurological function.<sup>1</sup>

The nuclear factor erythroid 2-related factor 2 (Nrf2) has been considered as an essential cytoprotective transcription factor regulating cellular redox balance and protective antioxidation.<sup>6</sup> Once the stressful conditions occur, Nrf2 is released from its inhibitor protein and translocates to the nucleus where it binds to anti-oxidative reagents elements, initiating the expression of a series of downstream protective genes.<sup>7,8</sup> Heme oxygenase (HO)-1 is one of the downstream proteins of Nrf2, and it is positively regulated by Nrf2.<sup>9–11</sup> Results from HO-1 knock-out animal models have indicated that HO-1 plays important roles in maintaining iron homeostasis and

\* Corresponding author at: Department of Critical Care Medicine, Renmin Hospital of Wuhan University, Wuhan, Hubei, China.

E-mail address: [yuzhui@whu.edu.cn](mailto:yuzhui@whu.edu.cn) (Z. Yu).

<https://doi.org/10.1016/j.resplu.2024.100703>

Received 11 March 2024; Received in revised form 16 June 2024; Accepted 17 June 2024

reducing oxidative stress damage.<sup>12</sup> As the rate-limiting enzyme in heme degradation, HO-1 catalyzes the heme into carbon monoxide (CO), biliverdin, and free iron.<sup>13</sup> HO-derived CO, out of all the byproducts of heme degradation, arises as a potential therapy for anti-inflammatory, anti-oxidative, and anti-apoptotic conditions based on preclinical and clinical studies.<sup>14,15</sup>

Much effort has been dedicated to prove the benefits of HO-1 and HO-derived CO in the setting of IRI, independently or in combination.<sup>16–18</sup> Inhalation CO has been used in clinical practice, however, its intense attraction to hemoglobin and subsequent formation of carboxyhemoglobin can have detrimental effects on the transportation of oxygen to the tissues.<sup>19</sup> Carbon monoxide-releasing molecule (CORM)-3, a water-soluble CORM, has been proven to be an effective carrier to deliver CO in a controlled manner while avoiding the side effects of potential toxicity of inhaled CO.<sup>20,21</sup> It is also reported that CORMs could up-regulate HO-1 expression.<sup>22–24</sup> The effect of CORM-3 on neuroprotection has been investigated in several disease models, including hemorrhagic stroke, traumatic brain injury, and spinal cord injury,<sup>18,25–30</sup> but not in cerebral IRI induced by CA/CPR. PCABI is the leading cause of death in patients who are resuscitated from CA, however, few studies have investigated the effect of CORM-3 in such patients.

The purpose of this study was to explore whether CORM-3 administration could improve survival and neurological outcomes after CA/CPR in mice. Additionally, we conducted additional investigations into the alterations in the permeability of the brain-blood barrier (BBB) and CBF, changes of oxidative stress level, the extent of neuroinflammation and neuronal death, and the activation of Nrf2/HO-1 signaling pathway.

## Materials and methods

All experiments were conducted in adherence to the Guide for the Care and Use of Laboratory Animals (NIH, United States) and approved by the Institutional Animal Care and Use Committee of Renmin Hospital of Wuhan University (No. WDRM 20171204).

### Animals

Male C57/BL6 mice (8–10 weeks old) were obtained from Hunan SJA Laboratory Animal Co., Ltd and housed in the Animal Experiment Center of Renmin Hospital of Wuhan University until surgery. Mice had access to food and water ad libitum and were housed in a 12-hour cycle, and a constant room temperature of  $22 \pm 1$  °C.

### Randomization

Mice were randomly allocated to four groups: 1) Sham + Vehicle; 2) CA/CPR + Vehicle; 3) Sham + CORM-3; 4) CA/CPR + CORM-3. Allocation was block-randomized 1:1 using a computer-generated randomization program by an investigator (ZY).

### Sample size and power estimates

Based on our previous experience as the mean survival rate at 72 h after CA/CPR was expected as 20% and 70% after CORM-3 treated, we anticipated that 12 mice per group were required in survival analysis ( $\alpha = 0.05$ ,  $\beta = 0.2$  [Power = 80%], two-sided).

### Blinding

The investigator (ZY) prepared the drug and administered the drug. The content of the drug was only known to ZY to conceal group allocation. The neurological function assessment was performed by the designated investigator who did not know the group allocation. The statistical analysis was blinded to group allocation by the designated investigator. All other group members were also blinded to group allocation.

### Cardiac arrest and cardiopulmonary resuscitation animal model

A mice model combined asystole with hemorrhage was performed. CA/CPR operation was performed as previously described.<sup>31,32</sup> Briefly, tracheal intubation was performed after anesthesia induction with 4.5%–5.0% isoflurane, and anesthesia was maintained with 1.0%–1.5% isoflurane. Exhaust gas was collected by gas evacuation apparatus during anesthesia. A rodent ventilator was set to a tidal volume of 0.3–0.5 mL and connected to the tracheal cannula. The electrocardiogram (ECG) was monitored throughout the procedure. The body temperature was monitored by a rectal temperature probe and maintained at  $37.0$  °C  $\pm$   $0.2$  °C. A polyethylene catheter was inserted through the right jugular vein for drug delivery. Heparin (50  $\mu$ L, 5 U) was given via the right jugular vein was cannulated, and 300  $\mu$ L blood was drawn. CA was induced by infusing 30  $\mu$ L (0.5 M) potassium chloride (KCl), then mechanical ventilation (MV) was immediately ceased. CA was confirmed by the cessation of spontaneous respiration and ECG. Slowly reinfusing the 300  $\mu$ L blood at 3 min after successful CA onset. Resuscitation was initiated at 9.5 min following CA onset by resuming MV with 100% O<sub>2</sub>, stopping warming, and infusing a dose of epinephrine (100  $\mu$ L, 32  $\mu$ g/ml) followed by continuous pumping at 20  $\mu$ L/min till 150  $\mu$ L. ROSC was characterized by sustained and stable ECG sinus rhythms. Resuscitation was stopped if ROSC was not achieved within 4 min, or spontaneous breath was not achieved within 16 min, and the mouse was excluded from the experiment. Carefully closed the wound, disconnected from MV, and transferred the mice into a thermal incubator (32.0 °C) for 2 h before returning to cages. The schematic CA/CPR animal model is shown in Fig. 1A. Typical ECG waveforms was presented in Fig. 1B.

### Drug administration and experimental design

Compound CORM-3 (SML 0496, Sigma) was dissolved in normal saline and administered intraperitoneally at 1 h after the ROSC in a dose of 30 mg/kg. Mice in the sham group experienced vehicle (normal saline) infused rather than KCl after the catheter was inserted. The schematic diagram of the experimental process is shown in Fig. 1C.

### Neurologic function and motor function assessment

#### Neurologic scores

Neurological dysfunction was evaluated with a 12-point scoring system.<sup>33</sup> Mice were scored by their performance on 6 sections: 1) level of consciousness; 2) corneal reflex; 3) spontaneous breathing; 4) righting reflex; 5) coordination; 6) activity (2 points for each section, 0 = severe impairments, 12 = normal).

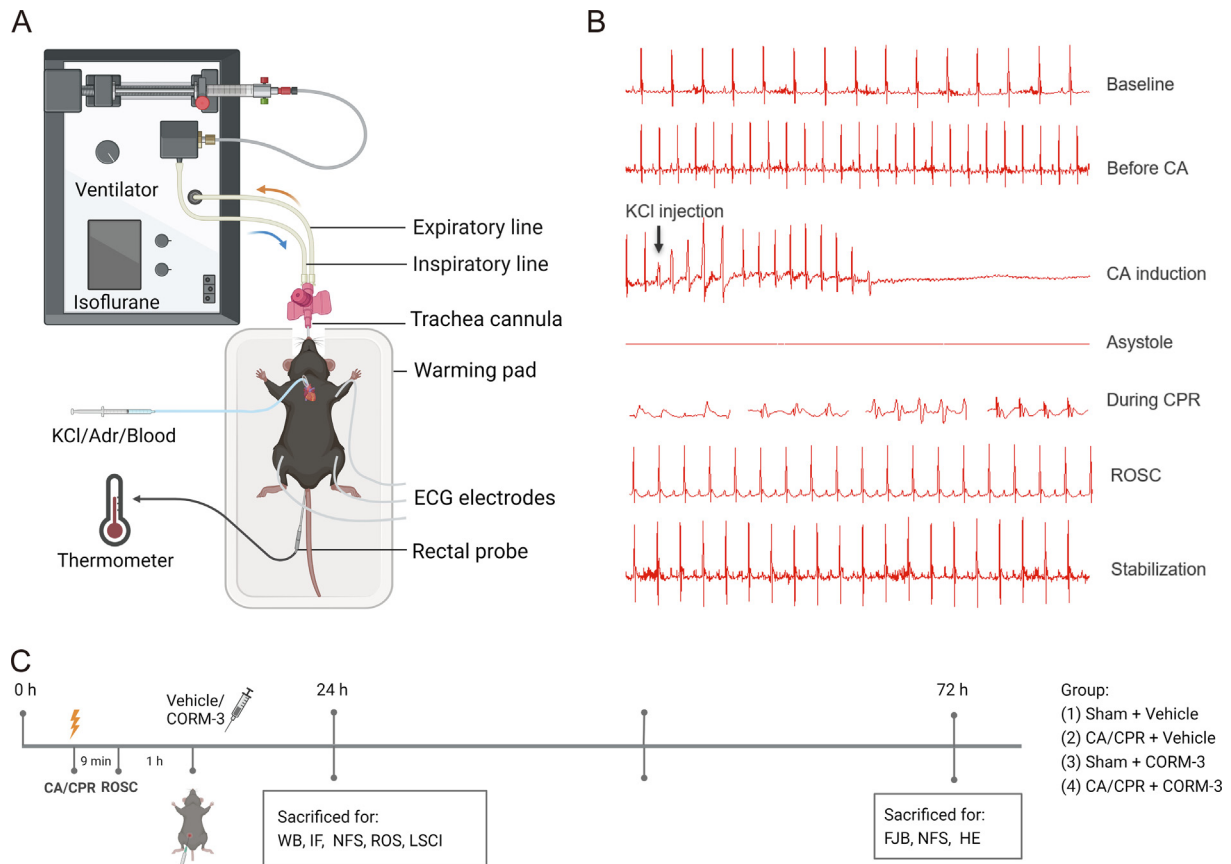


**Fig. 1 – Experiment schematic diagram and study timeline. (A) The schematic diagram of the operation showed the general procedures of the operation, including respiratory management, anesthesia management, temperature control, ECG monitoring, jugular vein separation and catheter insertion, and drug injection. (B) Electrocardiograph (ECG) was monitored during the surgery and typical ECG waveforms were recorded. (C) Mice were subjected to a 9.5-min cardiac arrest followed by cardiopulmonary resuscitation (CA/CPR) or a sham operation without CA induction. Vehicle (normal saline) or CORM-3 (a carbon monoxide-releasing molecule, 30 mg/kg) with an equal volume were intraperitoneally injected at 1 h after ROSC. The effect of CORM-3 on neurological function, brain-blood barrier (BBB), cerebral blood flow (CBF), oxidative stress injury, and activation of Nrf2/HO-1 signaling pathway were detected at 24 h after CA/CPR or sham operation. The effect of CORM-3 on neurological function, motor function, neuroinflammation and neuron death were detected at 72 h after CA/CPR or sham operation. Groups: (1) Sham + Vehicle; (2) CA/CPR + Vehicle; (3) Sham + CORM-3; (4) CA/CPR + CORM-3. CA, cardiac arrest; CPR, cardiopulmonary resuscitation; ROSC, return of spontaneous circulation; WB, Western blotting; IF, Immunofluorescent; HE, Hematoxylin-eosin; FJB, Fluoro-Jade B; LSCI, Laser specklecontrast imaging; DHE, Dihydroethidium; NFS, neurological function score; ROS, reactive oxygen species; BBB, brain-blood barrier; CBF, cerebral blood flow; ECG, electrocardiograph.**

#### Motor scores

Motor dysfunction was assessed by a 9-point scoring system.<sup>34</sup> Mice were scored by their performance on three sections: 1) vertical mash; 2) horizontal bar; 3) rope (0–3 points for each test, 0 = severe impairments, 9 = normal).

#### Motor scores of hindlimb

Movement of the hindlimb was evaluated by a 4-point score (0 represent completely paralyzed, and 4 represents for normal).<sup>35</sup>

#### Hematoxylin-eosin staining

Neuronal aberrant morphology was detected by Hematoxylin-eosin (HE) staining. Mice were anesthetized and intracardially perfused

with cold PBS (4 °C), followed by 4% paraformaldehyde to obtain brain tissue. After being fixed in 4% paraformaldehyde, the brain was dehydrated, embedded in paraffin, and sliced into coronal slices. The sections were deparaffinized and blocked, stained with hematoxylin and eosin, and then visualized by Olympus microscopy. The cell counting was performed by Image J software.

#### Fluoro-Jade B staining

Fluoro-Jade B (FJB) staining was performed to investigate the degeneration of neurons. The brain sections prepared previously were deparaffinized dewaxing to water. FJB working liquid (1:400, Millipore) was dropped, and diluted FJB green fluorescent probe was added, and stayed overnight at 4 °C. The slides were viewed

under the Olympus microscope, and the number of FJB-positive cells in the cortex area was manually counted. The fluorescence intensity and cell counting were measured by Image J software.

### **Laser speckle contrast imaging**

Laser speckle contrast imaging (LSCI, Moor Instruments) was applied to monitor global CBF (a key component of brain hemodynamics) as previously described.<sup>36,37</sup> Four mice of each group at 24 h after CA/CPR were tested. Mice were anesthetized with isoflurane, and body temperature was monitored and maintained at 33 °C. The skull was exposed by making a middle scalp incision and covered with normal saline. The same imaging parameters were used in all mice: flux image (lower: 50, upper: 2500, palette: 256 color palette1), frame rate (frequency: 50 Hz), duration (free run for 6 s). The signal intensities of CBF (Flux value) in the region of interest (whole brain) were measured with moorO2Flo-2, version 1.0 (Moor Instruments).

### **Immunofluorescent staining**

The coronal brain sections prepared previously were deparaffinized and rehydrated. The coronal brain sections were circled after antigen repairment and 3% BSA to block it for 30 min. Primary antibodies from different sources were mixed, the prepared primary antibodies were dripped, and the slices were laid flat in a wet box for incubation at 4 °C overnight. The corresponding secondary antibody was added conjugated to Alexa Fluor 488 (GB25303, Servicebio) or Alexa Fluor 594 (111-585-003, Jackson) for 1 h at 37 °C, then incubated at room temperature (RT) for 1 h in the dark. The primary antibodies used were listed as follows: mouse anti-gial fibrillary acidic protein (GFAP, 3670, Cell Signaling Technology) and rabbit anti-ionized calcium-binding adaptor molecule 1 (Iba1, 17198, Cell Signaling Technology), rabbit anti-Nrf2 (1:500, #12721, Cell Signaling Technology), rabbit anti-HO-1 (1:2500, ab68477, Abcam). Images were detected and collected by Fluorescent Microscopy. The fluorescence intensity was measured by Image J software.

### **Detection of reactive oxygen species generation**

The reactive oxygen species (ROS) generation was measured by dihydroethidium (DHE) staining.<sup>38–40</sup> The brain sections were frozen in liquid nitrogen before embedding in an OCT embedding medium and slicing up to fresh frozen coronal sections. After being incubated with DHE staining solution (D7008, Sigma) for 30 min at 37 °C away from light, the sections were imaged by the Olympus microscope. The fluorescence intensity was measured by ImageJ software.

### **Western blotting**

The mice were sacrificed at 24 h after CA/CPR or sham operation for western blotting analysis. Mice cortex tissues were homogenized in ice-cold lysis buffer supplemented with protease inhibitors. The homogenates were centrifuged at 14,000 × *g* for 10 min to remove cellular debris. The lysates were diluted with 5 × loading buffer (G2013, Servicebio) and boiled at 95 °C for 5 min, followed by separated by sodium dodecyl sulfate–polyacrylamide gel electrophoresis (SDS-PAGE) using 10–12% glycine gels. Proteins on the gels were transferred to polyvinylidene difluoride membranes (0.45 μm, Millipore). Membranes were blocked in free quick blocking buffer (PS108P, Epizyme) for 20 min at RT and then stained with primary antibodies at 4 °C overnight. The membranes were washed five 5-min with Tris-buffered saline (TBS) with 0.1% Tween-20 (TBST) and incubated with appropriated horseradish peroxidase (HRP)-

conjugated secondary antibodies for 1 h at RT. After five 5-min washes, the protein bands were visualized by ECL Kit (HY-K1005, MedChemExpress) and captured by an imaging system (Bio-rad). Image densitometry analyses were quantified using Image J software. The primary antibodies used in this study were: mouse anti-β-actin (1:1000, #3700, Cell Signaling Technology), rabbit anti-Nrf2 (1:500, #12721, Cell Signaling Technology), rabbit anti-HO-1 (1:2500, ab68477, Abcam), rabbit anti-Claudin-1 (1:2000, 28674-1, Proteintech), rabbit ZO-1 (1:2000, 21773-1, Proteintech). The primary antibodies were diluted by primary antibody dilutions (G2025, Servicebio). The secondary antibodies used were: HRP goat anti-rabbit (IgG) (1:10000, AS014, ABclonal), HRP goat anti-mouse (IgG) (1:10000, AS003, ABclonal). The secondary antibodies were diluted in 5% nonfat milk/TBST. Membranes were horizontally cut to probe proteins with different molecular weights.

### **Statistical analysis**

Data are presented as mean ± standard (SD), and *P* value < 0.05 were considered as statistically significant differences. Differences among more than 2 groups were assessed using one-way ANOVA with Tukey's post hoc test, and differences between two groups were assessed using the two-tail Students *t*-test. GraphPad Prism 8.0 software was used to perform data analysis (GraphPad Software, La Jolla, CA).

## **Results**

### **CORM-3 treatment improved survival and neurological function while decreasing body weight loss after CA/CPR**

Forty-eight mice (*n* = 12/group) were successfully included in the final analysis, and the overall assignment of mice for specific experiments was shown in Supplementary Table 1. There was no significant difference in variables at baseline and during CA/Sham operation among the four groups (*P* > 0.05 for each, see supplementary Table 2 for detail). A significantly decreased mortality in mice treated with CORM-3 relative to vehicle at 24 h (58.33% vs. 75.00%, *P* = 0.0146) and 72 h (16.67% vs. 66.67%, *P* < 0.0001) was observed (Fig. 2A). Since an overall improved status in eating after careful observation of mice was found, we evaluated body weight loss of mice at 24 h after surgery and found a notable decrease in body weight loss after CORM-3 treatment (mean body weight loss, CA/CPR + Vehicle vs. CA/CPR + CORM-3, 3.46 g vs. 1.30 g; *P* = 0.003, Fig. 2B). Additionally, we used both neurological and motor score systems to perform a comprehensive assessment of the mice's condition 24 h and 72 h after operation. Based on the 12-point scoring system, mice receiving CA/CPR without intervention showed worse neurological damage, while those treated with CORM-3 presented improved neurologic function at 24 h and 72 h (*P* < 0.05 for each, Fig. 2C–D). Likewise, mice treated with CORM-3 also showed improved motor function and hindlimb function scoring system as well (Fig. 2E–F).

### **CORM-3 treatment reduced neuronal apoptosis and attenuated neuroinflammation after CA/CPR**

FJB staining and HE staining were performed at 72 h to investigate whether CORM-3 treatment could reduce neuroinflammation and neurodegeneration. As shown in Fig. 3A, FJB-positive cells were reduced after CORM-3 treated (CA/CPR + Vehicle vs. CA/CPR + CORM-3, *P* = 0.0008), indicating less neurodegeneration.

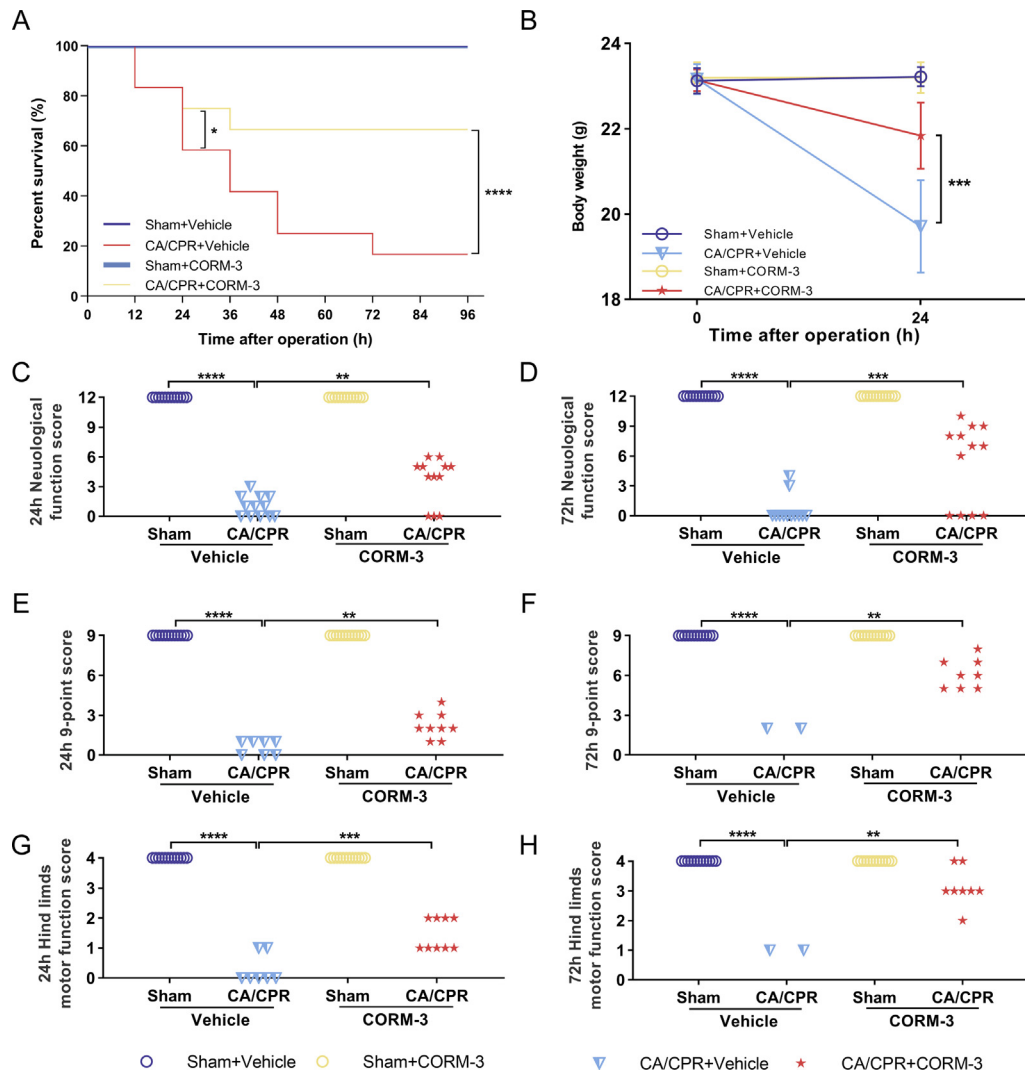


**Fig. 2 – Effects of CORM-3 on survival, neurological and motor function, and body weight. (A) Kaplan-Meier survival plots showed a significantly improved survival rate in CA/CPR + CORM-3 group compared with CA/CPR + Vehicle group (n = 12/group). (B) Significant reduction of weight loss in CA/CPR + CORM-3 group compared with CA/CPR + Vehicle group. (C-D) Results of 12-point neurological score. (E-F) 9-point score and (G-H) hind limb motor function score systems at 24 h and 72 h after CA/CPR, respectively. Results indicated a poor neurological and motor function at 24 h and 72 h after CA/CPR, which were significantly improved after CORM-3 administered. Dead mice were excluded from statistical analysis. Data are presented as mean ± SD. \*,  $P < 0.05$ ; \*\*,  $P < 0.01$ ; \*\*\*,  $P < 0.001$ ; \*\*\*\*,  $P < 0.0001$ .**

Likewise, results of HE staining showed severe neuron injury after CA/CPR which was reduced with CORM-3 treatment after operation (CA/CPR + Vehicle vs. CA/CPR + CORM-3,  $P = 0.0017$ , Fig. 3B). Combined with the results of neurological function and motor function assessment, CORM-3 significantly reduced neurodegeneration and improved neural function recovery. Furthermore, IF staining for GFAP/Iba-1 was used to evaluate the level of neuroinflammation. In comparison with vehicle-treated CA/CPR mice, CORM-3-treated mice had significantly reduced Iba-1 and GFAP expression ( $P = 0.0122$  and  $P = 0.0416$ , respectively, Fig. 3D-E), indicating alleviated neuroinflammation. Thus, CORM-3 may attenuate neuron degeneration and neuroinflammation to some extent in PCABI.

#### **CORM-3 treatment increases CBF of the cerebral cortex**

LSCI was used to evaluate CBF at 24 h after operation. Markedly reduced CBF after CA/CPR was observed (sham + Vehicle vs. CA/CPR + Vehicle,  $P = 0.0038$ ), and the CBF was slightly increased after CORM-3 treatment compared with vehicle treatment in PCABI mice ( $P = 0.0038$ , Fig. 4A).

#### **CORM-3 treatment reduced BBB leakage after CA/CPR**

We investigated the expression of tight junction (TJs) proteins to explore the BBB function. Western blotting analysis observed decreased expression of ZO-1 and Claudin-1 following CA/CPR, indicating disrupted BBB integrity. However, this tendency of BBB

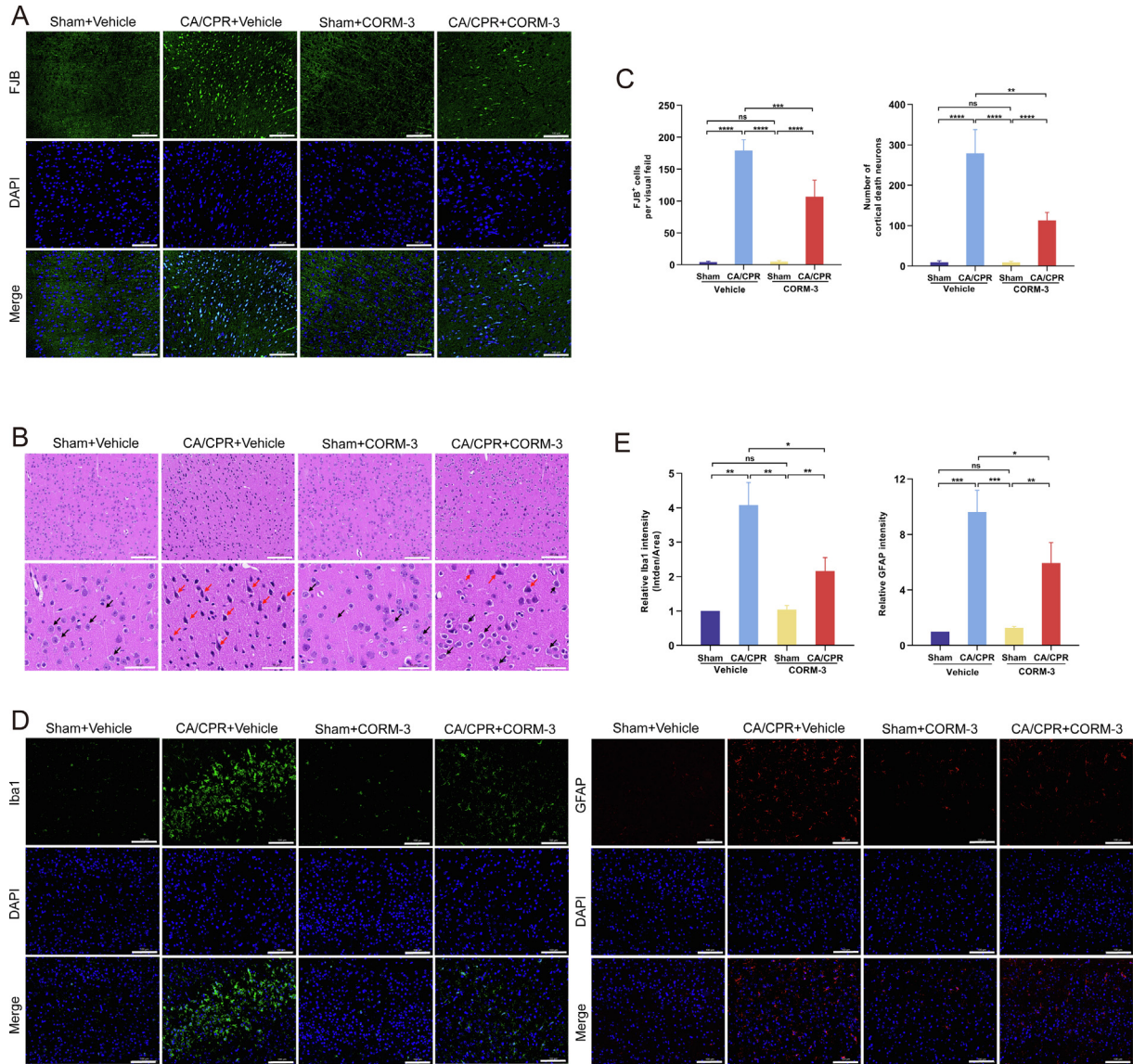


**Fig. 3 – Effects of CORM-3 on neuropathological damage and neuroinflammation after CA/CPR.** FJB and HE staining were used to evaluate neuropathological damage, while IF staining was used to evaluate neuroinflammation 72 h following CA/CPR or a sham operation. (A) Representative photomicrographs of FJB staining in the cortex; (B) Representative photomicrographs of HE staining in the cortex; (C) Quantification of FJB-positive cells and counts of death neurons; (D) Representative photomicrographs of Iba1 and GFAP in the cortex; (E) Semi-quantitative results of Iba1 and GFAP staining. Black arrows indicate the normal neurons and red arrows indicate dead neurons in HE staining. Results demonstrated that neuroinflammation and neuronal death were reduced after CORM-3 treatment. Scale bar, 100  $\mu$ m. Data are presented as mean  $\pm$  SD (n = 4/group). \*,  $P < 0.05$ ; \*\*,  $P < 0.01$ ; \*\*\*,  $P < 0.001$ ; \*\*\*\*,  $P < 0.0001$ ; ns, no significant. CA, cardiac arrest; CPR, cardiopulmonary resuscitation; FJB, Fluoro-Jade B; HE, Hematoxylin-eosin; IF, Immunofluorescent. (For interpretation of the references to color in this figure legend, the reader is referred to the web version of this article.)

damage was significantly alleviated after CORM-3 was treated, as indicated by increased ZO-1 (CA/CPR + Vehicle vs. CA/CPR + CORM-3,  $P = 0.0037$ ) and Claudin-1 (CA/CPR + Vehicle vs. CA/CPR + CORM-3,  $P = 0.0046$ ) protein expression (Fig. 4B). Taken together, it is reasonable to suppose that CORM-3 contributes to decreasing the loss of expression of TJs proteins.

#### **CORM-3 treatment attenuated the production of ROS**

We detected the ROS production to explore whether CORM-3 could attenuate oxidative stress. As shown in Fig. 5A, ROS generation was significantly stimulated after CA/CPR (sham + Vehicle vs. CA/CPR + Vehicle,  $P < 0.0001$ ), while CORM-3 treatment attenuated this response (CA/CPR + Vehicle vs. CA/CPR + CORM-3,

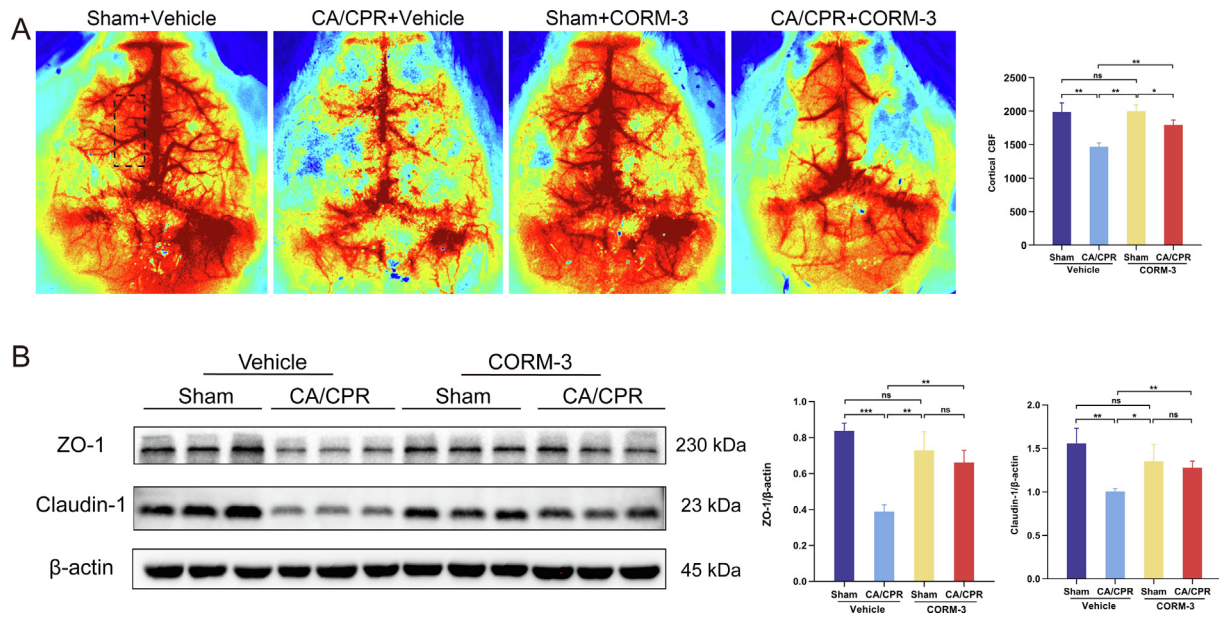


**Fig. 4 – Effects of CORM-3 on cerebral blood flow and brain-blood barrier function after CA/CPR.** Laser speckle contrast imaging (LSCI) was used to monitor cerebral blood flow (CBF) in the cortex at 24 h after CA/CPR or sham operation. **(A)** Representative photomicrographs of LSCI and quantitative CBF measurement of the cortical areas by LSCI. The regions for quantification were marked with dashed rectangles. CBF change was calculated by comparing to the sham group. **(B)** Western blotting analysis of ZO-1 and Claudin-1 in the cortex. Results showed that CBF in the cortex was significantly reduced after CA/CPR, while increased after CORM-3 treatment. In addition, the expression of ZO-1 and Claudin-1 was increased after CORM-3 treatment, indicating enhanced BBB integrity. Data are presented as mean ± SD (n = 4/group). \*,  $P < 0.05$ ; \*\*,  $P < 0.01$ ; \*\*\*,  $P < 0.001$ ; \*\*\*\*,  $P < 0.0001$ ; ns, no significant; CBF, cerebral blood flow; LSCI, Laser speckle contrast imaging; BBB, brain – blood barrier.

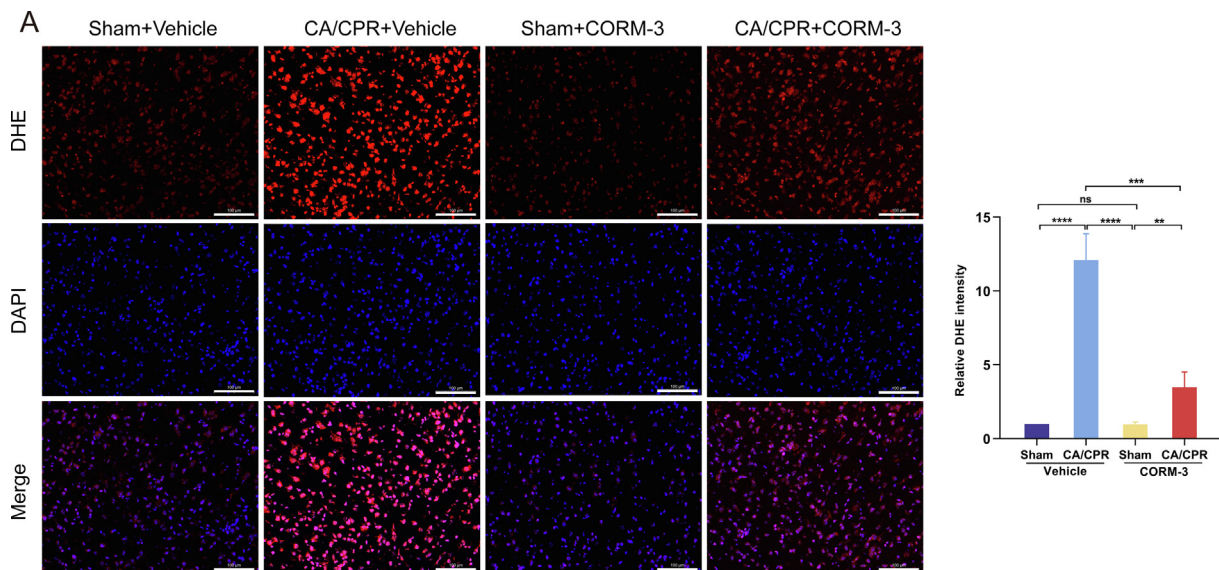


**Fig. 5 – Effects of CORM-3 on ROS production after CA/CPR.** **(A)** DHE staining was used to evaluate ROS production in the cortex and semi-quantitative results of DHE. Results showed that the ROS production was significantly elevated after CA/CPR, but further alleviated after CORM-3 was administered. Scale bar = 100 μm. Data are presented as mean ± SD (n = 4/group). \*\*,  $P < 0.01$ ; \*\*\*,  $P < 0.001$ ; \*\*\*\*,  $P < 0.0001$ ; ns, no significant; ROS, reactive oxygen species; DHE, dihydroethidium.

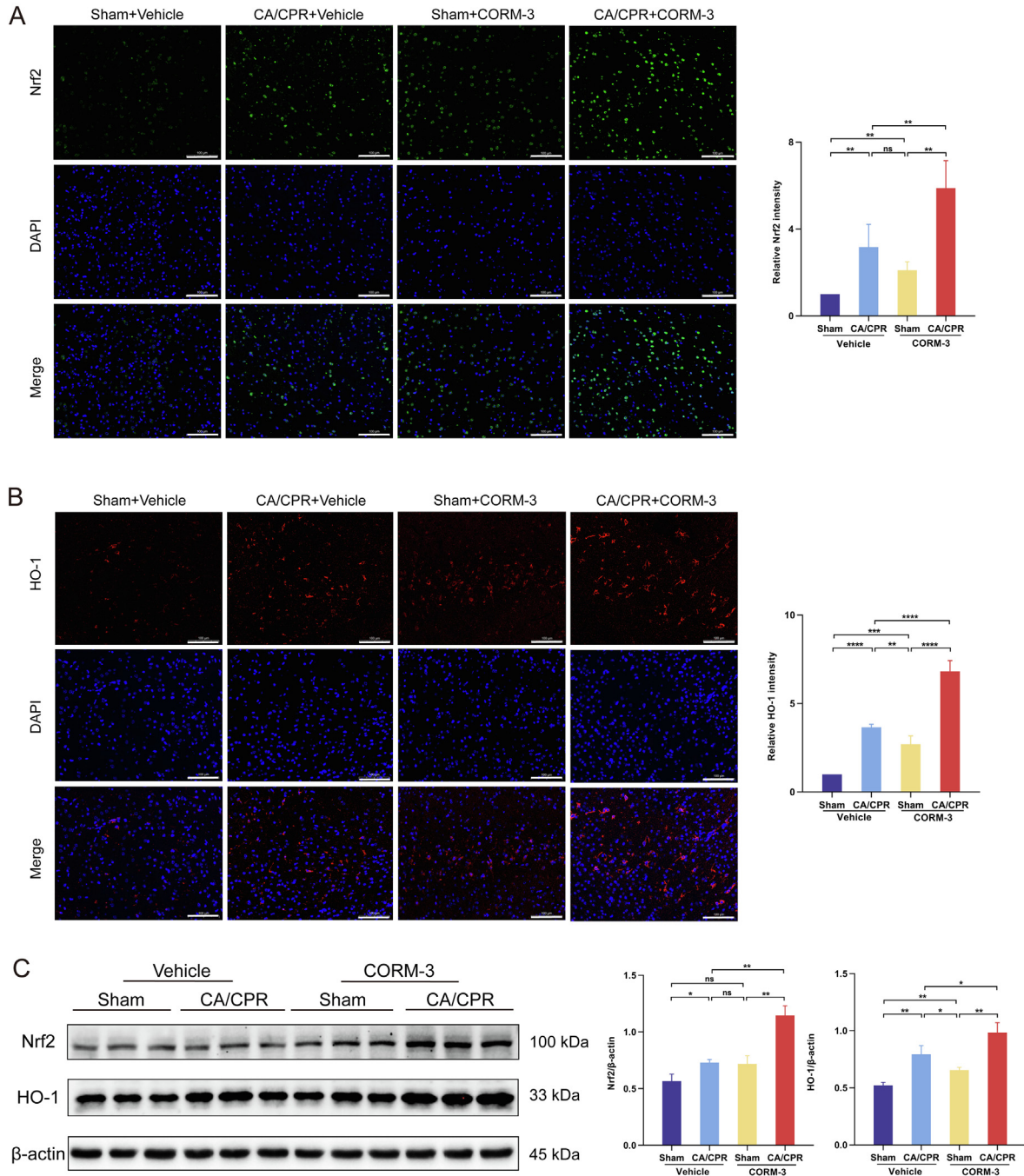


**Fig. 6 – Effects of CORM-3 on the activation of Nrf2/HO-1 signaling pathway. (A) Representative photomicrographs of Nrf2 by IF staining and semi-quantitative staining; (B) Representative photomicrographs of HO-1 by IF staining and semi-quantitative staining; (C) Western blotting analysis of Nrf2 and HO-1. Scale bar = 100  $\mu$ m. Data are presented as mean  $\pm$  SD (n = 4/group). \*,  $P < 0.05$ ; \*\*,  $P < 0.01$ ; \*\*\*,  $P < 0.001$ ; \*\*\*\*,  $P < 0.0001$ ; ns, no significant; IF, Immunofluorescent.**

$P = 0.0002$ ). The result indicated that CA/CPR-mediated cerebral oxidative stress was relieved by CORM-3.

#### **CORM-3 treatment activated Nrf2/HO-1 signaling pathway**

The vital protective effect of Nrf2 and its downstream molecule, HO-1, in IRI has been documented. In several of disease models,

CORM-3 has been found to reduce IRI by activating Nrf2/HO-1 signaling pathway. Thus, we further evaluated the activity of Nrf2/HO-1 signaling pathway after CORM-3 was administered. Results of IF staining showed a slight increase of Nrf2 expression in Sham + CORM-3 group compared with Sham + Vehicle group ( $P = 0.0013$ , Fig. 6A). Likewise, slight activation of Nrf2 was found



in mice who experienced CA/CPR while treated with vehicle (sham + Vehicle vs. CA/CPR + Vehicle,  $P = 0.0062$ ). That is to say, Nrf2 expression could be stimulated to some extent by both CA/CPR operation and CORM-3 administration. It is worth noting that the simultaneous implementation of CA/CPR and CORM-3 administration significantly enhanced Nrf2 activation (CA/CPR + Vehicle vs. CA/CPR + CORM-3,  $P = 0.0164$ ). Similar changes were found in HO-1 expression, as shown in Fig. 6B ( $P < 0.05$  for each). Western blotting results verified that maximal Nrf2/HO-1 signaling pathway activation achieved by CORM-3 intervention following CA/CPR ( $P < 0.05$  for each, Fig. 6C). Based on our findings, it can be deduced that even though CA/CPR could induce a partial activation of the Nrf2/HO-1 signaling pathway, it failed to provide sufficient protection against PCABI. CORM-3 administration after CA/CPR could induce an overactivation of Nrf2/HO-1 signaling pathway, leading to a more pronounced benefit on neuroprotection and survival.

## Discussion

The major findings of the present experiment showed that intraperitoneal injection of CORM-3 to mice with PCABI could improve survival and promote neurological function recovery. Besides, CORM-3 played a role in increasing CBF, reducing ROS generation, alleviated TJs degradation and mitigating neuronal injuries on PCABI. These benefits might be associated with activating Nrf2/HO-1 signaling pathway.

The mechanisms related to PCABI involve not only impaired CBF and oxygen supply, but also the IRI that occurs after ROSC. Cerebral IRI contributes to neuronal death and neuroinflammation, which aggravate neuronal damage and have detrimental effects on both short-term and long-term prognosis.<sup>1,41,42</sup> Microglia is considered as a major cellular contributor to neuroinflammation by producing cytokines to aggravate brain damage.<sup>25,43,44</sup> Previous research has demonstrated the neuroprotective advantages of CORMs-derived CO in animal models of spinal cord injury, traumatic brain injury, transient middle cerebral artery occlusion, and brain astrocyte cell line.<sup>18,26,45,46</sup> Our findings verified that CORM-3 could alleviate neuroinflammation and neuro death after CA/CPR. In addition, according to our observation of the survival status of mice, mice subjected to CORM-3 treatment exhibited independent eating and drinking behavior after 12 h post-operation, which was supported by less weight loss assessed at 24 h after surgery. Furthermore, a thorough evaluation of neurological and motor function conducted at both 24 h and 72 h time points presented expected beneficial outcomes in CA mice treated with CORM-3. Collectively, we demonstrated that the administration of CORM-3 has the potential to improve both neurological function recovery in PCABI.

Being an organ characterized by high metabolism and high oxygen consumption, the brain contains a limited capacity for energy restoration. Thus, it relies on a relatively stable CBF to ensure a constant supply of oxygen and an effective removal of metabolic by-products. Both inhaled CO and CORM-3 have been proven to have positive effects on vasodilation and anti-adhesion of cells to the endothelial resulting in maintenance of blood flow in disease models such as kidney transplantation, lung transplantation, and spontaneously hypertensive.<sup>47–50</sup> We observed a marked reduction of blood flow in the cortex region after CA/CPR as compared to the sham group as results of LSCI presented. An apparent notable augmentation in CBF was discovered in mice subjected to CORM-3

treatment. This finding suggested that the administration of CORM-3 may cause cerebral vasodilation, subsequently leading to an increase in CBF.

Deterioration in BBB function may play a key role in the pathogenesis of PCABI.<sup>51,52</sup> TJs constitute the junction complex of the BBB. Claudins-1 plays an important role in the generation of TJs forming the BBB in the brain.<sup>53,54</sup> It develops connections with cytoplasmic proteins, including ZO-1, to create a solid cytoplasmic bridge.<sup>55</sup> CORM-3 treatment has been reported to restore BBB integrity by increasing the expression of TJs proteins and reducing Evans blue leakage after transient middle cerebral artery occlusion.<sup>25</sup> Similarly, by lessening ZO-1 degeneration and neutrophil infiltration, CORM-3 also lessened the deterioration of the spinal cord-blood barrier in a mouse model of spinal cord injury.<sup>30</sup> In the present study, we measured alterations in BBB permeability by analyzing the expression of barrier function markers (ZO-1 and Claudin-1) which have been verified by previous studies showing that they could represent changes in BBB permeability.<sup>56,57</sup> Our findings match those observed in the previous studies, reporting that markers of barrier function were decreased after CA/CPR but significantly alleviated after CORM-3 was administered, indicating that CORM-3 helps to alleviate the BBB dysfunction. Moreover, oxidative stress injury could also lead to BBB dysfunction. A previous study has reported that CORM-A1 helped preserve BBB functional integrity damaged by inotropic glutamate receptor-mediated endothelial oxidative stress and apoptosis.<sup>58</sup> Detection of alterations in blood composition has been proposed as an alternative way to predict BBB disruption.<sup>59,60</sup> Additional research might focus on identifying bloodstream markers that could serve as an alternative for evaluating BBB dysfunction.

Free radical formation, endothelial dysfunction, intracellular  $Ca^{2+}$  overload, and excitatory neurotransmitter releasing aggravate brain injury after reperfusion. Given that an over-activated oxidative stress response is associated with irreversible damage of neurons, we detected the generation of ROS induced by IRI.<sup>61</sup> Results from studies in organ transplantation models demonstrated beneficial effects with CORM-3 treated in terms of enhanced preservation of organs and improved vasodilatory effects, especially a diminished response to oxidative stress.<sup>62,63</sup> We have demonstrated that CA/CPR induced oxidative stress and ER stress in the hippocampus in the previous study.<sup>31</sup> The current in vivo experiment revealed an increased generation of ROS in the cerebral cortex of mice subjected to CA/CPR, further confirming that IRI after ROSC is a robust inducer of oxidative stress to the whole brain. ROS production was observed to be significantly reduced in the presence of CORM-3, suggesting that CORM-3 effectively mitigated oxidative stress. Taken together, we considered that attenuating oxidative stress might be a potential way for CORM-3 to exert neuroprotection in PCABI. Additional experiments are needed to explore how CORM-3 influences oxidative stress reaction, and the relationship between CORM-3 and mitochondrial function.

Nrf2/HO-1 signaling pathway is considered a major regulator of antioxidation and intracellular redox homeostasis.<sup>6</sup> A previous study reported that activation of Nrf2/HO-1 signaling pathway alleviated oxidative stress and pro-inflammatory response to limit oxidative damage.<sup>64</sup> In addition, we also found that activation of Nrf2/HO-1 signaling pathway could attenuate endoplasmic reticulum stress and exert neuroprotective effects along with ATF6 signaling pathway in PCABI.<sup>31</sup> Though there are similarities between our two research in terms of enhanced activity of Nrf2/HO-1 signaling pathway after CA/CPR, however, level of Nrf2/HO-1 signaling pathway activity after

CA/CPR could not exert sufficient neuroprotection of PCABI in the present study. That could be an explanation for high mortality and poor neurological performance in mice that only suffer CA/CPR but without CORM-3 treated. A notable activation of the Nrf2/HO-1 signaling pathway after the administration of CORM-3 and the consistent prognosis further verified our hypothesis. Although our experimental results showed that CORM-3-induced overactivation of Nrf2/HO-1 signaling pathway may play critical roles in mitigating PCABI, gene knockdown in vivo did not be performed in the current study. Therefore, further research is needed to explore the protective mechanisms of CORM-3 more extensively.

There were several limitations of our study. First, we only investigated the impacts of CORM-3 on brain injury in a group of young male adult mice. The effects of CORM-3 on female and aged mice may need to be fully elucidated. Second, CORM-3 given through intraperitoneal injection with a bolus dosage at 1 h after operation. Further research should consider other intravenous injection strategies and different time points of drug administration to fully account for the potential influence of delivery routes on the effects of CORM-3. Third,  $n = 4$ /group of samples were included in brain tissue analysis due to consideration of limiting animal use numbers, larger sample size should be considered in the future study. Moreover, we used a mice model combined asystole with hemorrhage together which made the induction and severity of CA complicated. Additional hemodynamic and cardiac function parameters are needed to provide more accurate hemodynamic monitoring. Lastly, malnutrition and postoperative weakness may be confounding in neurological deficiency, additional experiments are needed to explore the impacts of confounding on neurological function.

## Conclusion

In conclusion, we demonstrated that CORM-3 treatment could improve survival and exert neuroprotection after CA/CPR in mice. The neuroprotective effects might be attributed to the activation of Nrf2/HO-1 signaling pathway. CORM-3 may be a novel and promising drug target of PCABI.

## Ethics approval and consent to participate

All experimental procedures were performed in adherence to the Guide for the Care and Use of Laboratory Animals (NIH, United States) and approved by the Institutional Animal Care and Use Committee of Renmin Hospital of Wuhan University (No. WDRM 20171204).

## CRedit authorship contribution statement

**Yuanrui Zhao:** Writing – original draft, Visualization, Software, Formal analysis, Conceptualization. **Zhun Yao:** Visualization, Methodology, Investigation. **Liping Lu:** Supervision, Data curation. **Song Xu:** Writing – review & editing. **Jianfei Sun:** Methodology. **Ying Zhu:** Methodology. **Yanping Wu:** Methodology. **Zhui Yu:** Supervision, Funding acquisition, Data curation.

## Data availability statement

The data of this research are available upon reasonable request to the corresponding author.

## Declaration of competing interest

The authors declare that they have no known competing financial interests or personal relationships that could have appeared to influence the work reported in this paper.

## Acknowledgments

Zhu Yuan made contributions to animal model establishment. The graphical figures were created by Biorender.com.

## Author contributions

YR-Z conceptualized, performed the study, wrote the original draft, and created Figs. 1-2 as well as graphic abstract. YZ performed animal model establishment, visualized and edited the Figs. 3-6. JF-S, YP-W and YZ performed behavioral experiments. LP-L supervised the study implementation and examined the data. SX reviewed the manuscript. ZY reviewed the data and approved the manuscript. All authors reviewed the manuscript.

## Funding

The work was supported by National Natural Science Foundation of China (No. 81772039) and the Knowledge Innovation Program Project of Wuhan Municipal Science and Technology Bureau (No. 2022020801010474).

## Appendix A. Supplementary data

Supplementary data to this article can be found online at <https://doi.org/10.1016/j.resplu.2024.100703>.

## Author details

<sup>a</sup>Department of Critical Care Medicine, Renmin Hospital of Wuhan University, Wuhan, China <sup>b</sup>Central Laboratory, Renmin Hospital of Wuhan University, Wuhan, China

## REFERENCES

- Perkins GD, Callaway CW, Haywood K, et al. Brain injury after cardiac arrest. *Lancet* (London, England) 2021;398:1269–78. [https://doi.org/10.1016/s0140-6736\(21\)00953-3](https://doi.org/10.1016/s0140-6736(21)00953-3).
- Chaban V, Nakstad ER, Stær-Jensen H, et al. Complement activation is associated with poor outcome after out-of-hospital cardiac arrest. *Resuscitation* 2021;166:129–36. <https://doi.org/10.1016/j.resuscitation.2021.05.038>.

3. Mentzelopoulos SD, Zakynthinos SG. Post-cardiac arrest syndrome: pathological processes, biomarkers and vasopressor support, and potential therapeutic targets. *Resuscitation* Dec 2017;121:A12–4. <https://doi.org/10.1016/j.resuscitation.2017.10.013>.
4. Jeong S, Pollin KU, DuBose LE, et al. Brain blood flow: The more you N.O.. *J Phys* 2022;600:11–3. <https://doi.org/10.1113/jp282475>.
5. Fan JL, Brassard P, Rickards CA, et al. Integrative cerebral blood flow regulation in ischemic stroke. *J Cereb Blood Flow Metab* 2022;42:387–403. <https://doi.org/10.1177/0271678x211032029>.
6. Dodson M, de la Vega MR, Cholanians AB, et al. Modulating NRF2 in disease: Timing is everything. *Annu Rev Pharmacol Toxicol* 2019;59:555–75. <https://doi.org/10.1146/annurev-pharmtox-010818-021856>.
7. Zhang DD, Hannink M. Distinct cysteine residues in Keap1 are required for Keap1-dependent ubiquitination of Nrf2 and for stabilization of Nrf2 by chemopreventive agents and oxidative stress. *Mol Cell Biol* 2003;23:8137–51. <https://doi.org/10.1128/mcb.23.22.8137-8151.2003>.
8. Uruno A, Yamamoto M. The KEAP1-NRF2 system and neurodegenerative diseases. *Antioxid Redox Signal* 2023;38:974–88. <https://doi.org/10.1089/ars.2023.0234>.
9. Campbell NK, Fitzgerald HK, Dunne A. Regulation of inflammation by the antioxidant haem oxygenase 1. *Nat Rev Immunol* 2021;21:411–25. <https://doi.org/10.1038/s41577-020-00491-x>.
10. Consoli V, Sorrenti V, Grosso S, et al. Heme Oxygenase-1 Signaling and Redox Homeostasis in Physiopathological Conditions. *Biomolecules* 2021;11. <https://doi.org/10.3390/biom11040589>.
11. Loboda A, Damulewicz M, Pyza E, et al. Role of Nrf2/HO-1 system in development, oxidative stress response and diseases: an evolutionarily conserved mechanism. *Cell Mol Life Sci* 2016;73:3221–47. <https://doi.org/10.1007/s00018-016-2223-0>.
12. Yachie A. Heme Oxygenase-1 deficiency and oxidative stress: a review of 9 independent human cases and animal models. *Int J Mol Sci* 2021;22. <https://doi.org/10.3390/ijms22041514>.
13. Liu R, Yang J, Li Y, et al. Heme oxygenase-1: The roles of both good and evil in neurodegenerative diseases. *J Neurochem* 2023;167:347–61. <https://doi.org/10.1111/jnc.15969>.
14. Ryter SW. Therapeutic Potential of Heme Oxygenase-1 and Carbon Monoxide in Acute Organ Injury, Critical Illness, and Inflammatory Disorders. *Antioxidants (Basel)*. 2020; 9. doi: 10.3390/antiox9111153.
15. Motterlini R, Otterbein LE. The therapeutic potential of carbon monoxide. *Nat Rev Drug Discov* 2010;9:728–43. <https://doi.org/10.1038/nrd3228>.
16. Wu YH, Hsieh HL. Roles of heme oxygenase-1 in neuroinflammation and brain disorders. *Antioxidants (Basel)* 2022;11. <https://doi.org/10.3390/antiox11050923>.
17. Ryter SW, Choi AM. Targeting heme oxygenase-1 and carbon monoxide for therapeutic modulation of inflammation. *Transl Res* 2016;167:7–34. <https://doi.org/10.1016/j.trsl.2015.06.011>.
18. Zheng G, Zhan Y, Wang H, et al. Carbon monoxide releasing molecule-3 alleviates neuron death after spinal cord injury via inflammasome regulation. *EBioMedicine* Feb 2019;40:643–54. <https://doi.org/10.1016/j.ebiom.2018.12.059>.
19. Queiroga CS, Vercelli A, Vieira HL. Carbon monoxide and the CNS: challenges and achievements. *Br J Pharmacol* 2015;172:1533–45. <https://doi.org/10.1111/bph.12729>.
20. Xing CY, Tarumi T, Liu J, et al. Distribution of cardiac output to the brain across the adult lifespan. *J Cereb Blood Flow Metab* 2017;37:2848–56. <https://doi.org/10.1177/0271678x16676826>.
21. Yuan Z, Yang X, Wang B. Redox and catalase-like activities of four widely used carbon monoxide releasing molecules (CO-RMs). *Chem Sci* 2021;12:13013–20. <https://doi.org/10.1039/d1sc03832j>.
22. Lin CC, Yang CC, Hsiao LD, et al. Carbon monoxide releasing molecule-3 enhances heme oxygenase-1 induction via ROS-dependent FoxO1 and Nrf2 in brain astrocytes. *Oxid Med Cell Longev* 2021;2021:5521196. <https://doi.org/10.1155/2021/5521196>.
23. Idriss NK, Blann AD, Lip GY. Hemoxygenase-1 in cardiovascular disease. *J Am Coll Cardiol* 2008;52:971–8. <https://doi.org/10.1016/j.jacc.2008.06.019>.
24. Hirao H, Dery KJ, Kageyama S, et al. Heme Oxygenase-1 in liver transplant ischemia-reperfusion injury: From bench-to bedside. *Free Radic Biol Med* 2020;157:75–82. <https://doi.org/10.1016/j.freeradbiomed.2020.02.012>.
25. Wang J, Zhang D, Fu X, et al. Carbon monoxide-releasing molecule-3 protects against ischemic stroke by suppressing neuroinflammation and alleviating blood-brain barrier disruption. *J Neuroinflammation* 2018;15:188. <https://doi.org/10.1186/s12974-018-1226-1>.
26. Lin CC, Yang CC, Hsiao LD, et al. Heme oxygenase-1 induction by carbon monoxide releasing molecule-3 suppresses interleukin-1 $\beta$ -mediated neuroinflammation. *Front Mol Neurosci* 2017;10:387. <https://doi.org/10.3389/fnmol.2017.00387>.
27. Li Y, Zhang LM, Zhang DX, et al. CORM-3 ameliorates neurodegeneration in the amygdala and improves depression- and anxiety-like behavior in a rat model of combined traumatic brain injury and hemorrhagic shock. *Neurochem Int* 2020;140:104842. <https://doi.org/10.1016/j.neuint.2020.104842>.
28. Zhang LM, Zhang DX, Fu L, et al. Carbon monoxide-releasing molecule-3 protects against cortical pyroptosis induced by hemorrhagic shock and resuscitation via mitochondrial regulation. *Free Radic Biol Med* 2019;141:299–309. <https://doi.org/10.1016/j.freeradbiomed.2019.06.031>.
29. Al Mamun A, Wu Y, Monalisa I, et al. Role of pyroptosis in spinal cord injury and its therapeutic implications. *J Adv Res* 2021;28:97–109. <https://doi.org/10.1016/j.jare.2020.08.004>.
30. Zheng G, Zheng F, Luo Z, et al. CO-releasing molecule (CORM)-3 ameliorates spinal cord-blood barrier disruption following injury to the spinal cord. *Front Pharmacol* 2020;11:761. <https://doi.org/10.3389/fphar.2020.00761>.
31. Yuan Z, Lu L, Lian Y, et al. AA147 ameliorates post-cardiac arrest cerebral ischemia/reperfusion injury through the co-regulation of the ATF6 and Nrf2 signaling pathways. *Front Pharmacol* 2022;13:1028002. <https://doi.org/10.3389/fphar.2022.1028002>.
32. Liu H, Yu Z, Li Y, et al. Novel modification of potassium chloride induced cardiac arrest model for aged mice. *Aging Dis* 2018;9:31–9. <https://doi.org/10.14336/ad.2017.0221>.
33. Hayashida K, Bagchi A, Miyazaki Y, et al. Improvement in outcomes after cardiac arrest and resuscitation by inhibition of S-nitrosoglutathione reductase. *Circulation* 2019;139:815–27. <https://doi.org/10.1161/circulationaha.117.032488>.
34. Shen Y, Yan B, Zhao Q, et al. Aging is associated with impaired activation of protein homeostasis-related pathways after cardiac arrest in mice. *J Am Heart Assoc* 2018;7:e009634.
35. Ahn JH, Lee TK, Kim B, et al. Therapeutic hypothermia improves hind limb motor outcome and attenuates oxidative stress and neuronal damage in the lumbar spinal cord following cardiac arrest. *Antioxidants (Basel)* 2020;9. <https://doi.org/10.3390/antiox9010038>.
36. Li R, Duan W, Zhang D, et al. Mouse cardiac arrest model for brain imaging and brain physiology monitoring during ischemia and resuscitation. *J Visualiz Exp: JoVE*. 2023. doi:10.3791/65340.
37. Junyun H, Hongyang L, Ruoxian D, et al. Real-time monitoring of cerebral blood flow by laser speckle contrast imaging after cardiac arrest in rat. *Annual International Conference of the IEEE Engineering in Medicine and Biology Society IEEE Engineering in Medicine and Biology Society Annual International Conference* 2015;2015:6971–4. <https://doi.org/10.1109/embc.2015.7319996>.
38. Sang D, Lin K, Yang Y, et al. Prolonged sleep deprivation induces a cytokine-storm-like syndrome in mammals. *Cell* 2023;186:5500–5516.e21. <https://doi.org/10.1016/j.cell.2023.10.025>.
39. Lu L, Jang S, Zhu J, et al. Nur77 mitigates endothelial dysfunction through activation of both nitric oxide production and anti-oxidant pathways. *Redox Biol* 2024;70:103056. <https://doi.org/10.1016/j.redox.2024.103056>.

40. Du H, Ma Y, Wang X, et al. Advanced glycation end products induce skeletal muscle atrophy and insulin resistance via activating ROS-mediated ER stress PERK/FOXO1 signaling. *Am J Phys Endocrinol Metab* 2023;324:E279–87. <https://doi.org/10.1152/ajpendo.00218.2022>.
41. Sekhon MS, Ainslie PN, Griesdale DE. Clinical pathophysiology of hypoxic ischemic brain injury after cardiac arrest: a “two-hit” model. *Crit Care*. 2017; 21: 90. doi: 10.1186/s13054-017-1670-9.
42. Jurcau A, Simion A. Neuroinflammation in cerebral ischemia and ischemia/reperfusion injuries: from pathophysiology to therapeutic strategies. *Inter J Molecul Sci* 2021;23. <https://doi.org/10.3390/ijms23010014>.
43. Zhang Z, Zhang Z, Lu H, et al. Microglial Polarization and Inflammatory Mediators After Intracerebral Hemorrhage. *Mol Neurobiol* 2017;54:1874–86. <https://doi.org/10.1007/s12035-016-9785-6>.
44. Ousta A, Piao L, Fang YH, et al. Microglial activation and neurological outcomes in a murine model of cardiac arrest. *Neurocrit Care* 2022;36:61–70. <https://doi.org/10.1007/s12028-021-01253-w>.
45. Zhang LM, Zhang DX, Zheng WC, et al. CORM-3 exerts a neuroprotective effect in a rodent model of traumatic brain injury via the bidirectional gut-brain interactions. *Exp Neurol* 2021;341:113683. <https://doi.org/10.1016/j.expneurol.2021.113683>.
46. Wollborn J, Steiger C, Doostkam S, et al. Carbon monoxide exerts functional neuroprotection after cardiac arrest using extracorporeal resuscitation in pigs. *Crit Care Med* 2020;48:e299–307. <https://doi.org/10.1097/ccm.0000000000004242>.
47. Foresti R, Hammad J, Clark JE, et al. Vasoactive properties of CORM-3, a novel water-soluble carbon monoxide-releasing molecule. *Br J Pharmacol* 2004;142:453–60. <https://doi.org/10.1038/sj.bjp.0705825>.
48. Failli P, Vannacci A, Di Cesare ML, et al. Relaxant effect of a water soluble carbon monoxide-releasing molecule (CORM-3) on spontaneously hypertensive rat aortas. *Cardiovasc Drugs Ther* 2012;26:285–92. <https://doi.org/10.1007/s10557-012-6400-6>.
49. Nakao A, Faleo G, Nalesnik MA, et al. Low-dose carbon monoxide inhibits progressive chronic allograft nephropathy and restores renal allograft function. *Am J Physiol Renal Physiol* 2009;297:F19–26. <https://doi.org/10.1152/ajprenal.90728.2008>.
50. Kohmoto J, Nakao A, Stolz DB, et al. Carbon monoxide protects rat lung transplants from ischemia-reperfusion injury via a mechanism involving p38 MAPK pathway. *Am J Transplant Off J Am Soc Transplant Am Soc Transplant Surg* 2007;7:2279–90. <https://doi.org/10.1111/j.1600-6143.2007.01940.x>.
51. Park JS, You Y, Min JH, et al. Study on the timing of severe blood-brain barrier disruption using cerebrospinal fluid-serum albumin quotient in post cardiac arrest patients treated with targeted temperature management. *Resuscitation* 2019;135:118–23. <https://doi.org/10.1016/j.resuscitation.2018.10.026>.
52. Kang C, You Y, Ahn HJ, et al. Blood-brain barrier disruption as a cause of various serum neuron-specific enolase cut-off values for neurological prognosis in cardiac arrest patients. *Sci Reports* 2022;12:2186. <https://doi.org/10.1038/s41598-022-06233-4>.
53. Furuse M, Sasaki H, Tsukita S. Manner of interaction of heterogeneous claudin species within and between tight junction strands. *J Cell Biol* 1999;147:891–903. <https://doi.org/10.1083/jcb.147.4.891>.
54. Liebner S, Fischmann A, Rascher G, et al. Claudin-1 and claudin-5 expression and tight junction morphology are altered in blood vessels of human glioblastoma multiforme. *Acta Neuropathol* 2000;100:323–31. <https://doi.org/10.1007/s004010000180>.
55. Kadry H, Noorani B, Cucullo L. A blood-brain barrier overview on structure, function, impairment, and biomarkers of integrity. *Fluids and Barriers of the CNS* 2020;17:69. <https://doi.org/10.1186/s12987-020-00230-3>.
56. Wu VM, Huynh E, Tang S, et al. Brain and bone cancer targeting by a ferrofluid composed of superparamagnetic iron-oxide/silica/carbon nanoparticles (earthicles). *Acta Biomater* 2019;88:422–47. <https://doi.org/10.1016/j.actbio.2019.01.064>.
57. Lee HL, Kim JM, Go MJ, et al. Fermented protaetia brevitarsis larvae improves neurotoxicity in chronic ethanol-induced-dementia mice via suppressing AKT and NF- $\kappa$ B signaling pathway. *Inter J Molec Sci* 2024;25. <https://doi.org/10.3390/ijms25052629>.
58. Basuroy S, Leffler CW, Parfenova H. CORM-A1 prevents blood-brain barrier dysfunction caused by ionotropic glutamate receptor-mediated endothelial oxidative stress and apoptosis. *Am J Physiol Cell Physiol* 2013;304:C1105–15. <https://doi.org/10.1152/ajpcell.00023.2013>.
59. Mercier E, Boutin A, Lauzier F, et al. Predictive value of S-100 $\beta$  protein for prognosis in patients with moderate and severe traumatic brain injury: systematic review and meta-analysis. *BMJ (Clinical Research ed)* 2013;346. <https://doi.org/10.1136/bmj.f1757>.
60. Shemilt M, Boutin A, Lauzier F, et al. Prognostic value of glial fibrillary acidic protein in patients with moderate and severe traumatic brain injury: a systematic review and meta-analysis. *Crit Care Med* 2019;47:e522–9. <https://doi.org/10.1097/ccm.0000000000003728>.
61. Granger DN, Kvietys PR. Reperfusion injury and reactive oxygen species: The evolution of a concept. *Redox Biol* 2015;6:524–51. <https://doi.org/10.1016/j.redox.2015.08.020>.
62. Obara T, Yamamoto H, Aokage T, et al. Luminal administration of a water-soluble carbon monoxide-releasing molecule (CORM-3) mitigates ischemia/reperfusion injury in rats following intestinal transplantation. *Transplantation* 2022;106(7):1365–75. <https://doi.org/10.1097/tp.0000000000004007>.
63. Katada K, Takagi T, Iida T, et al. Role and potential mechanism of heme oxygenase-1 in intestinal ischemia-reperfusion injury. *Antioxidants (Basel)* 2022;11. <https://doi.org/10.3390/antiox11030559>.
64. Vomund S, Schäfer A, Parnham MJ, et al. Nrf2, the Master Regulator of Anti-Oxidative Responses. *Int J Mol Sci* 2017;18. <https://doi.org/10.3390/ijms18122772>.